# Thermal depinning of fluxons in discrete Josephson rings

J. J. Mazo,[1,2] F. Naranjo,[1,2,3] and K. Segall[4]

[1]*Departamento de Física de la Materia Condensada, Universidad de Zaragoza, 50009 Zaragoza, Spain*
[2]*Instituto de Ciencia de Materiales de Aragón, CSIC-Universidad de Zaragoza, 50009 Zaragoza, Spain*
[3]*Universidad Pedagógica y Tecnológica de Colombia, Tunja, Colombia*
[4]*Department of Physics and Astronomy, Colgate University, Hamilton, New York 13346, USA*

We study the thermal depinning of single fluxons in rings made of Josephson junctions. Due to thermal fluctuations a fluxon can be excited from its energy minima and move through the array, causing a voltage across each junction. We find that for the initial depinning, the fluxon behaves as a single particle and follows a Kramers-type escape law. However, under some conditions this single-particle description breaks down. At low values of the discreteness parameter and low values of the damping, the depinning rate is larger than what the single-particle result would suggest. In addition, for some values of the parameters the fluxon can undergo low-voltage diffusion before switching to the high-voltage whirling mode. This type of diffusion is similar to phase diffusion in a single junction but occurs without frequency-dependent damping. We study the switching to the whirling state as well.

PACS number(s): 74.40.+k, 74.50.+r, 03.75.Lm, 74.81.Fa

## I. INTRODUCTION

In past years many works have been devoted to the study of extended discrete nonlinear systems. On one hand, it is important to deepen our knowledge on the general properties of such systems since they often have application to many different physical situations. On the other hand, many physical systems are well described by nonlinear discrete models. In this field, the emergence of the soliton concept for instance (in the continuous and its discrete counterparts) was paradigmatic.[1,2] A well-known example of a model system supporting this type of nonlinear excitations is the discrete sine-Gordon equation (also called Frenkel-Kontorova model).[3–5]

A Josephson-junction (JJ) array is, by construction, a discrete system made of interacting nonlinear solid-state devices. JJ arrays are an example of physical systems with great fundamental and technological interest which are well described by discrete nonlinear models.[6,7] From the experimental point of view, Josephson junctions are a privileged place to study solitons and to explore their possible applications.[8]

Among the many different geometries for a JJ array the so-called Josephson ring (a set of JJ connected in parallel in a closed array, forming a ring, see Fig. 1) is well described by a discrete sine-Gordon equation and supports nonlinear discrete solitons or kinks, usually called fluxons in this context.[9] Thus, many studies of the discrete sine-Gordon equation, or studies of the role of kinks in nonlinear arrays, have direct application when studying JJ rings. Conversely the study and modelization of JJ rings allow exploration of different issues concerning the behavior of these nonlinear phenomena.

Figure 1 shows a schematic of a Josephson ring with 9 junctions. When cooled below the superconducting critical temperature an integer number of magnetic-flux quanta, fluxons, can be trapped in the ring. Then, the physical properties of the array are dominated by the presence of the fluxons in

the system. The *I-V* curve of the array shows the mean voltage across the array as a function of a constant external current applied to every junction of the array. When current is applied, the array remains superconducting up to a certain critical value which defines the critical current of the array. In the presence of fluxons this current corresponds to the fluxon depinning current. At this current, the fluxon starts to move around the array and finite voltage is measured.

In many cases the energy exchange between the system and the environment is relevant, so thermal fluctuations have to be considered.[7] Because of this, at finite temperature the value of the depinning current and the shape of the *I-V* curve can be strongly affected by thermal fluctuations. Motivated by recent experiments on the thermal depinning and dynamics of fluxons (kinks) in small rings that are made of nine junctions,[10] in this work we numerically explore some of these issues. In addition, in some cases the fluxons can be understood as particles on a substrate periodic potential.

The main objective of this paper is to study numerically the thermal depinning of a single fluxon in a JJ ring and compare it with numerical simulations and analytical predictions for the case of a single particle. We have found excellent agreement in many cases. However, under some conditions the single-particle description fails. In addition, for
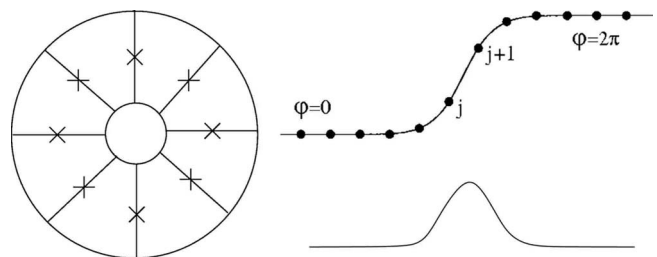


FIG. 1. Left: scheme of the JJ ring with planar geometry. Lines are for superconducting wires and crosses are for Josephson junctions. Right: phase configuration profile (top) and magnetic flux (bottom) for a fluxon in JJ ring.
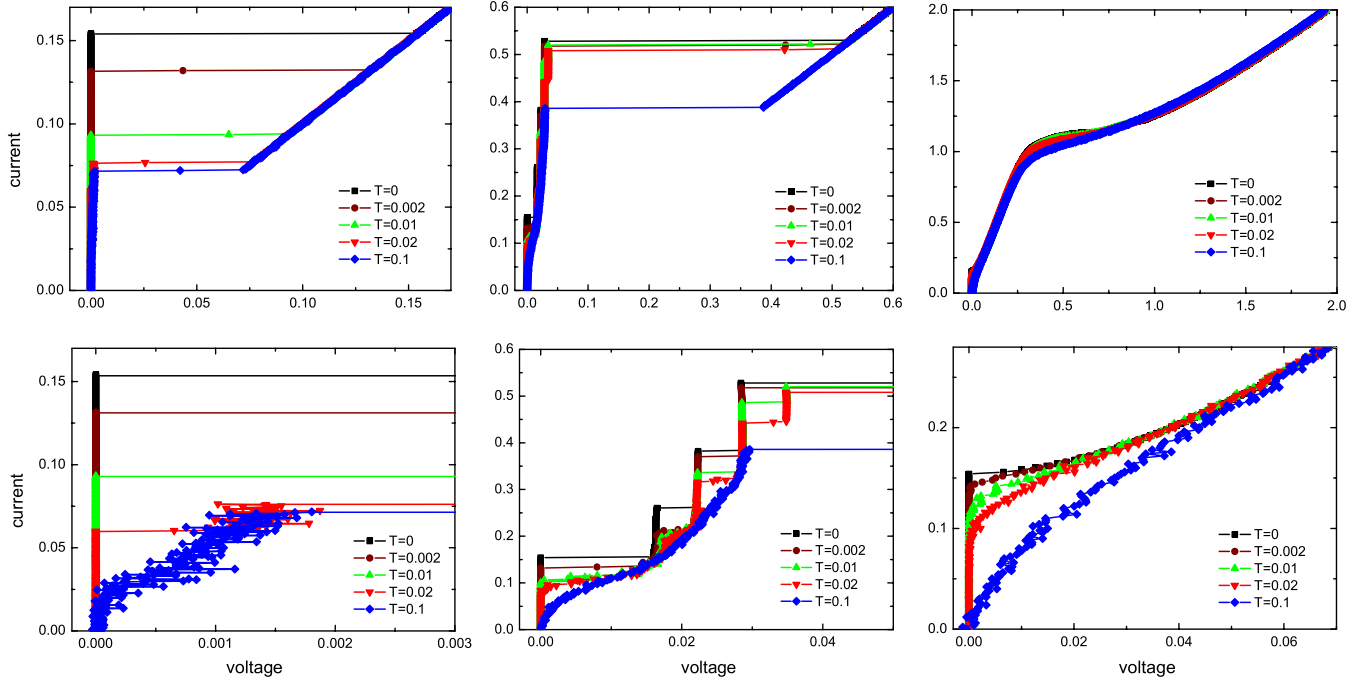
174510-1

FIG. 2. (Color online) *I-V* curves for one fluxon in a nine-junction ring with $\lambda=0.4$ at $\Gamma=0.01$ (left), $\Gamma=0.1$ (middle), and $\Gamma=1.0$ (right). Each figure shows five different temperatures ($T=0, 0.002, 0.01, 0.02, 0.1$).

some values of the parameters the fluxon can undergo low-voltage diffusion before switching to the high-voltage whirling mode. This type of diffusion is similar to phase diffusion in a single underdamped junction but occurs without frequency-dependent damping.

## II. EQUATIONS

Josephson junctions are made of two superconducting materials separated by a thin insulating barrier. Driven by an external current, this system behaves as a solid-state nonlinear oscillator and is modeled by the same dynamical equations that describe a driven pendulum:[7] $i=\ddot{\varphi}+\Gamma\dot{\varphi}+\sin\varphi+\xi(\tau)$. Here $\varphi$, the variable that describes the behavior of the junction, is the gauge-invariant phase difference of the superconducting order parameter at both sides of the junction. In this equation current is normalized by the junction critical current ($I_c$) and time is normalized by the junction plasma frequency, $\omega_p=\sqrt{2\pi I_c/\Phi_0 C}$ ($\Phi_0=h/2e$ is the magnetic-flux quantum and $C$ is the junction capacitance). $\Gamma$ is an important parameter which measures the dissipation in the system ($\Gamma=\sqrt{\Phi_0/2\pi I_c CR^2}$, with $R$ as the effective resistance of the junction). The last term, $\xi(\tau)$, describes the effect of thermal noise in the dynamics (Johnson current noise) and satisfies $\langle\xi(\tau)\rangle=0$ and $\langle\xi(\tau)\xi(\tau')\rangle=2\Gamma T\delta(\tau-\tau')$, where we use $T$ for a normalized temperature $T=k_B T_{\text{exp}}/E_J$ (with $E_J$ as the Josephson energy $E_J=\Phi_0 I_C/2\pi$). The normalized dc voltage $v$, which gives the response of the system to the external current, is defined by $v=V_{\text{dc}}/I_c R=(\Phi_0/2\pi I_c R)\langle d\varphi/dt\rangle=\Gamma\langle d\varphi/d\tau\rangle$.

As previously stated, the JJ ring consists of a series of individual junctions connected in parallel. Such system can be thought of as a series of coupled pendula. Following the usual model for the system, the equations for an array made of $N$ coupled junctions driven by the same external current are given by[9]

$$\ddot{\varphi}_j + \Gamma\dot{\varphi}_j + \sin\varphi_j + \xi_j(\tau) = \lambda(\varphi_{j+1} - 2\varphi_j + \varphi_{j-1}) + i. \quad (1)$$

Index $j$ denotes different junctions and runs from 1 to $N$. The new parameter $\lambda$ accounts for the coupling between the junctions which, in the framework of this model, occurs between neighbors and has an inductive character $\lambda=\Phi_0/2\pi I_c L$, with $L$ as the self-inductance of every cell in the array. Boundary conditions are defined by the topology of the array (here we consider circular arrays) and the number $M$ of trapped fluxons in the system: $\varphi_{j+N}=\varphi_j+2\pi M$.

In this paper we will consider the case of a single fluxon. We have studied different sizes for the array, but here we will present results for an array made of nine junctions, which are similar to those being experimentally studied. We will also study different values of $\lambda$ and restrict our interest to underdamped arrays biased by a dc current at a broad range of temperatures.

## III. RESULTS

In this section we are going to present numerical simulations of the dynamics of one fluxon in a Josephson ring and one particle in a periodic potential. We will also show numerical calculations from single-particle thermal escape theory.

### A. *I-V* curves: Damping regimes

Figure 2 shows single *I-V* curves for one fluxon in a nine-junction Josephson ring with $\lambda = 0.4$. In this case the width of the fluxon is close to 2, so it is well localized in the array and discreteness effects are important.[11] Curves were simulated at three different values of damping and five temperatures. Current was increased from zero to some maximum at an average ramp equal to $\frac{8}{3} \times 10^{-7}$ (in normalized units).

Let us look first at the $T=0$ curves. If we start at zero bias, in all the cases the fluxon is pinned to the array until the so-called depinning current $i_{\text{dep}}^0$ is reached (for $\lambda = 0.4$, $i_{\text{dep}}^0 \simeq 0.155$). Above this current very different *I-V* characteristics are observed depending on the value of the damping.

At small damping the system switches from the $v=0$ state to a high-voltage ohmic state ($v=i$), where all the junctions rotate uniformly (whirling branch). The damping is so small that when the fluxon moves through the array it excites all the junctions to the high-voltage state. In this voltage state the fluxon is totally delocalized in the array. For clarity, we have shown only the curves for increasing current. If current is decreased from the high-voltage state the junctions retrap at a small value of the current (mostly defined by $\Gamma$). The curve is hysteretic and shows bistability for a wide range of currents.

At intermediate values of damping the dynamics is much more complex. Now the *I-V* curve shows a low-voltage region dominated by a series of steps which correspond to resonances between the fluxon velocity and the linear modes of the array. These resonances have been the object of great attention in the past.[9,12–17] For these currents the fluxon moves around the ring in a localized manner. This regime persists up to a given value of the current for which the fluxon reaches a high velocity and all the junctions switch to the high-voltage part of the curve. At moderate damping the *IV* curve can also be multistable with hysteresis loops on every step.

At high values of the damping dissipation governs the dynamics, multistability disappears, and the voltage increases from zero without discontinuities and jumps as soon as current reaches the depinning value. In this part of the curve a localized fluxon is moving around the ring and voltage is related with the fluxon velocity. For currents close to 1 (in normalized units), it starts the transient to another regime where the fluxon delocalizes and all the junctions rotate and contribute to the overall voltage in the array.[5]

Figure 2 also shows the dynamics of the array in the presence of thermal noise. As can be seen in the figure, the first thermal effect is that the fluxon depins at smaller currents. For small damping we find that if temperature is high enough, noise also induces a fluxon diffusion branch, which we will discuss later in this paper. At moderate damping, the low-voltage resonances are rounded, and at high-enough temperature voltage increases smoothly from zero to some value on the fluxon diffusion branch and then switches to the high-voltage region of the *I-V* curve. At high damping temperature causes a rounding of the curve.

We will study how temperature affects the *I-V* curve at low damping, since this is the case for the experimental system we are trying to model. Usually the depinning current is experimentally defined as the current for which measured voltage is above a certain threshold. We have followed the same definition in our simulations. This is a good definition in the low-damping and low-temperature regime where the system switches between two very different voltage values so a threshold independent current is expected. However, the election of the threshold voltage is not trivial. A small threshold can give problems at large temperatures where voltage fluctuations are also large. A large threshold is not a good choice since it ignores possible low-voltage states such as the fluxon diffusion one. If low-voltage states are present we can distinguish between the depinning current $i_{\text{dep}}$ and the switching current $i_{\text{sw}}$, where depinning marks the end of the superconducting state and switching marks the end of the transition to the high-voltage branch. At very high temperatures noise can reach the threshold level and first switching is suppressed. To study this issue we have used in our simulation three or five different thresholds and compared results for all of them.

### B. $\langle i_{\text{dep}}(T) \rangle$

The depinning current is a stochastic variable with a given probability distribution. We present results for the mean value of the depinning current $\langle i_{\text{dep}} \rangle$ and its standard deviation $\sigma$. Results were obtained after the numerical simulation of the dynamical equations of the system for 1000 samples. We used different values of damping $\Gamma$ (typically from 0.001 to 0.1) and coupling $\lambda$ (usually from 0.2 to 1.0). The number of junctions in the array is $N=9$. Another important parameter of the simulations is the current ramp; in our case this ramp changes from one simulation to another but it is of the order of $1 \times 10^{-7}$.

Figure 3 shows results for $\Gamma = 0.01$ and five different values of the coupling ($\lambda = 0.2$, 0.4, 0.6, 0.8, and 1.0). The main physical properties of the fluxon in the array change importantly with the value of $\lambda$. Thus, the zero-temperature depinning current of the array $i_{\text{dep}}^0$ decreases by a factor of 30 from $\lambda = 0.2$ to 1.0 (see Table I). In order to compare the five curves, in Fig. 3 both axes have been scaled by the value of the zero-temperature depinning current for every case.[18] We see that once scaled all curves are similar showing that in this range of parameters these results can be understood in a unified manner.

In the figure we see that $\langle i_{\text{dep}} \rangle$ decreases to zero as an effect of temperature. All the curves follow the same behavior, but at high temperatures the small $\lambda$ curves slightly deviate from the others. For temperatures of the order of the barrier, thermal fluctuations dominate the dynamics and the depinning current goes to zero. In fact, at high temperatures there is no good definition of depinning current since different thresholds may give different results. With respect to the standard deviation, we can see that it grows with $T^{2/3}$ as predicted by standard thermal activation theory and reaches a maximum at high temperatures, when $\langle i_{\text{dep}} \rangle$ has an inflection point close to $\langle i_{\text{dep}} \rangle \rightarrow 0$. Then the standard deviation decreases since all escape events happen in a narrow range of current values.
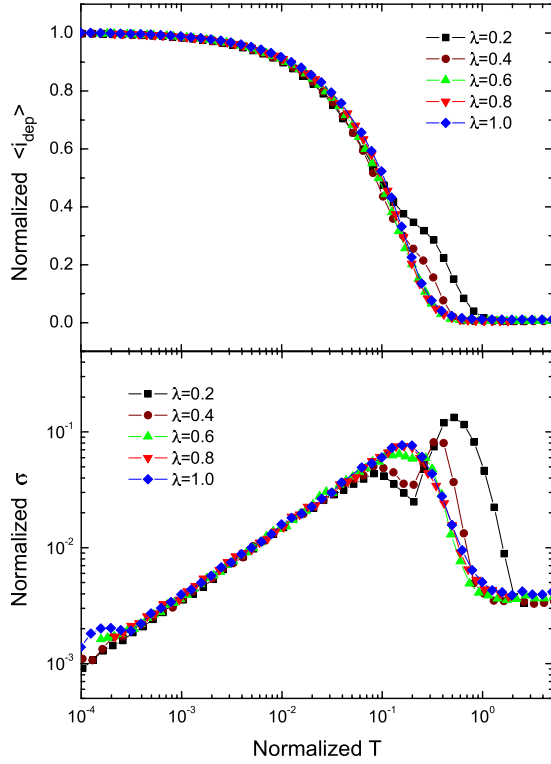
FIG. 3. (Color online) Numerical calculation of normalized $\langle i_{\text{dep}} \rangle$ and $\sigma$ versus normalized $T$ at $\Gamma = 0.01$ and five different values of $\lambda$ ($\lambda = 0.2, 0.4, 0.6, 0.8, 1.0$).

### C. Fluxon as a single particle

When studying the dynamics of one fluxon in the array it is very common to use the picture of this extended and collective object as a single particle.[3,4,19,20] This approach has been extensively used in the past and, as we will see, it is very useful although not exact.

Let us consider a new variable representing the center of masses of the fluxon or the position of the fluxon in the array. Then, in the simplest approach, the dynamics of a fluxon in a ring can be approached by the dynamics of a driven damped massive particle experiencing a sinusoidal substrate potential (Peierls-Nabarro potential) and subjected to thermal fluctuations,

$$m\ddot{X} + \Gamma m\dot{X} + i_{\text{dep}}^0 \sin X = i + \xi(\tau), \qquad (2)$$

where

$$\langle \xi(\tau) \rangle = 0 \quad \text{and} \quad \langle \xi(\tau)\xi(\tau') \rangle = 2m\Gamma T\delta(\tau - \tau'). \qquad (3)$$

TABLE I. Fluxon parameters at different values of $\lambda$.

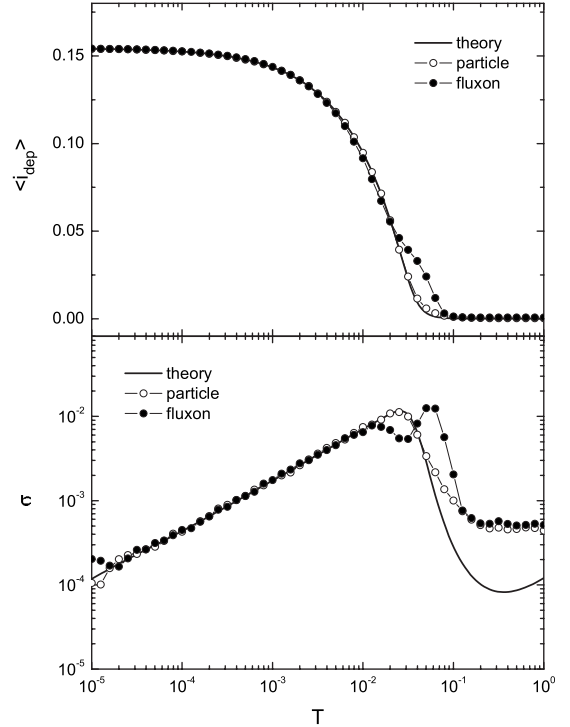| $\lambda$ | $E_{\text{PN}}$ | $\omega_{\text{PN}}^2$ | $m$ | $i_{\text{dep}}^0$ |
|-----------|-----------------|------------------------|-----|--------------------|
| 0.2 | 0.778 42 | 0.774 05 | 0.5028 | 0.384 82 |
| 0.4 | 0.309 74 | 0.447 75 | 0.3459 | 0.154 35 |
| 0.6 | 0.127 44 | 0.231 51 | 0.2757 | 0.063 67 |
| 0.8 | 0.055 39 | 0.117 21 | 0.2363 | 0.027 67 |
| 1.0 | 0.025 50 | 0.060 41 | 0.2110 | 0.012 725 |



FIG. 4. $\langle i_{\text{dep}} \rangle$ and $\sigma$ versus $T$ at $\Gamma = 0.01$ and $\lambda = 0.4$ for the fluxon; and a single particle in a periodic potential, and comparison with the theoretical prediction.

In this simple approach we are neglecting, for instance, the spatial dependence of the mass effective damping due to the other degrees of freedom of the system and higher-order terms in the expansion of the substrate potential for the fluxon. Table I gives a relation of numerically computed values of some of the parameters of the fluxon and its effective potential in the single-particle picture: $E_{\text{PN}}$ is the zero current potential barrier; $\omega_{\text{PN}}^2$ is the squared frequency for small amplitude oscillations of the fluxon around equilibrium; $m$ is the fluxon effective mass at rest (computed as $m = E_{\text{PN}}/2\omega_{\text{PN}}^2$), and $i_{\text{dep}}^0$ is the depinning current. For a perfect sinusoidal potential we should get $i_{\text{dep}}^0 = E_{\text{PN}}/2$. The exact results are close to it.

Figures 4 and 5 show, for lambda$= 0.4$ and $0.8$ (in both cases $\Gamma = 0.01$), the comparison between the results for the fluxon in the array, numerical simulations of the depinning of a single particle in a sinusoidal potential [Eq. (2)], and a theoretical calculation based on analytical results for the thermal activation rate of particles in sinusoidal potentials in the low-damping regime.[21–26] In the figure we plot the result computed from the Büttiker-Harris-Landauer equation for escape rate at $\alpha = 1$ [Eq. (3.11) in Ref. 23]. We have checked that a very close result (indistinguishable at the scale of the figure) is got when using $\alpha = 1.45$ (Ref. 27) or the Mel'nikov-Meshov theory.[24]

We can see that the single-particle simulations reproduce the results for the fluxon in an excellent way at this value of the damping in all the temperature range, although a small deviation in a range of temperatures is observed for $\lambda = 0.4$. Theoretical estimations disagree at high values of $T$ since escape rate equations were obtained in the infinite barrier limit ($E_b \gg k_B T$).
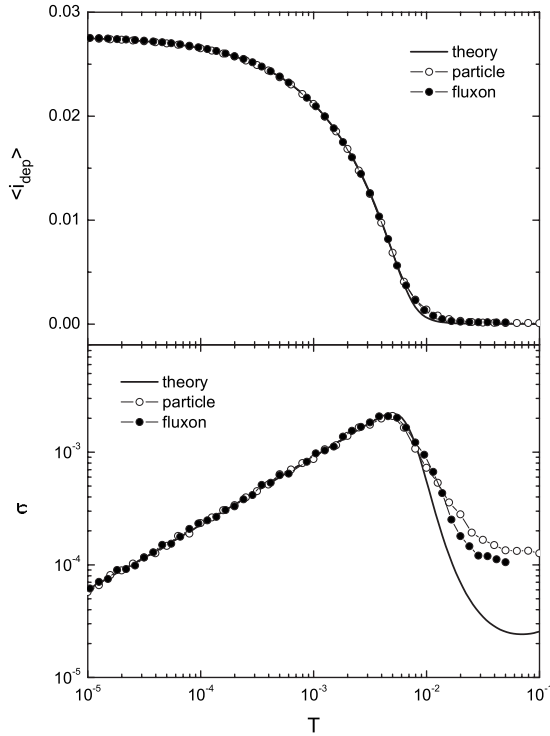
FIG. 5. $\langle i_{\text{dep}} \rangle$ and $\sigma$ versus $T$ at $\Gamma=0.01$ and $\lambda=0.8$ for the fluxon; and a single particle in a periodic potential, and comparison with the theoretical prediction.

The agreement shown in Figs. 4 and 5 does not occur for other values of coupling and damping. For instance, for $\lambda=0.4$ and $\Gamma=0.001$ (Fig. 9—below) a deviation of the simulated curve with respect to the theoretical prediction is found. To study further such result we have done numerical simulations at fixed $T$ for different values of $\Gamma$ and for $\lambda=0.4$ ($T=0.01$) and 0.8 ($T=0.0018$).[28] Results are shown in Figs. 6 and 7. There we can see that for $\lambda=0.4$ the fluxon results deviate importantly from that expected for the single particle (or the theory) when damping is decreased. However this is not the case for $\lambda=0.8$. In this respect the degree of discreteness of the system seems important. Such degree is measured by the coupling parameter $\lambda$ (high $\lambda$ approaches the continuum limit of the system, and small $\lambda$ increases the dis-
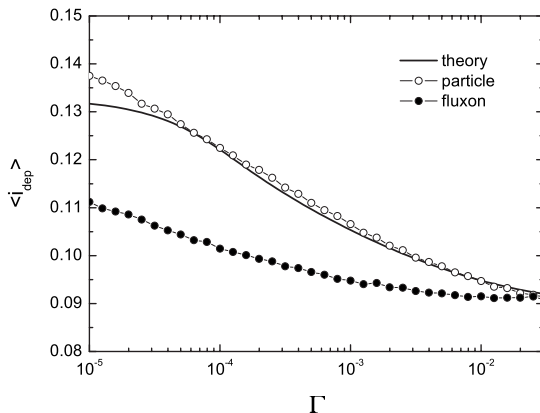


FIG. 6. $\langle i_{\text{dep}} \rangle$ as a function of $\Gamma$ for $\lambda=0.4$ at $T=0.01$.
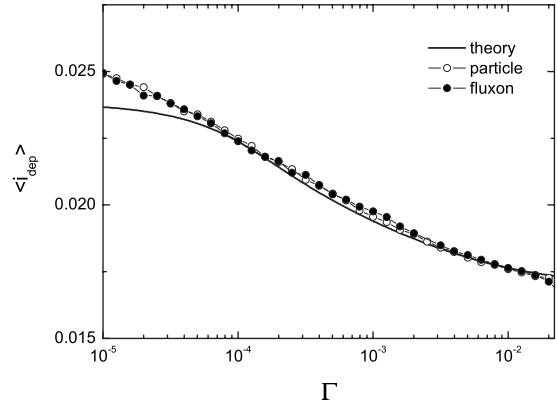


FIG. 7. $\langle i_{\text{dep}} \rangle$ as a function of $\Gamma$ for $\lambda=0.8$ at $T=0.0018$.

creteness effects). At small values of $\lambda$ effects due to other degrees of freedom are more important, and if damping is small such excitations persist longer in the system.

### D. Fluxon diffusion

In Fig. 2 we have seen that at low damping and high-enough temperature, a low-voltage branch appears in the $I$-$V$ curves before the escape to the full running state. In this low-voltage state, the transport of the fluxon occurs through a series of noise-induced $2\pi$ phase slips (or $2\pi/N$ depending on the definition of the fluxon center of masses), where every jump corresponds to a fluxon which advances one cell in the array. Such state cannot be understood in terms of the single-particle picture. In analogy with the phase diffusion that occurs in a single junction, we label this mode of transport fluxon diffusion. In spite of the fact that we are in the low-damping regime, the fluxon is able to travel along the ring without exciting the whirling branch. Remarkably this is a thermally excited state and it is not seen at low temperatures.

In Fig. 8 we show the time evolution of the phase of one junction (junction 1) and a phase associated with the center of mass of the fluxon defined as $\psi=\frac{1}{N}\Sigma_j\varphi_j$ to allow a better comparison. Current values have been chosen in the low-voltage branch. The random jumps of $2\pi$ for the junction or $2\pi/N$ for the fluxon phase $\psi$ are easily observed.

We have also done numerical experiments to simulate the jump from the diffusion branch to the full whirling state. These simulations are done with a higher voltage threshold but are otherwise similar to the previous experiments. Results for $\Gamma=0.01$ and $0.001$ are shown in Fig. 9, where $\lambda=0.4$. We see that theory and single-particle results agree quite well in all the ranges. At high-temperature thermal fluctuations dominate, of the order of the barrier, and theoretical results do not apply. We also see that the standard deviation increases with temperature, following the expected law up to a certain value where it reaches a maximum and then decreases when $\langle i_{\text{dep}} \rangle$ is close to zero.

However, in Fig. 9 we can also see that for the fluxon curve there exists a value of $T$ such that at higher temperatures, the value of the current for which the array switches to the whirling branch is temperature independent. This temperature shows the emergence of a fluxon diffusion branch in
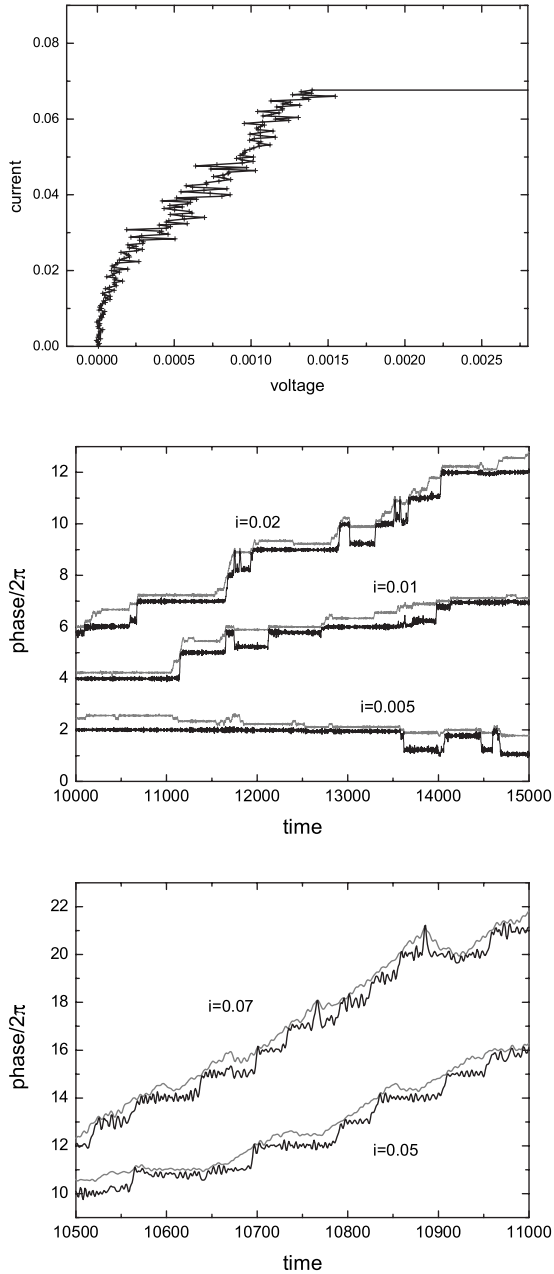
FIG. 8. $\lambda = 0.4$, $\Gamma = 0.01$, and $T = 0.1$. Top: *I-V* curve showing the small voltage fluxon diffusion branch. Medium and bottom: time evolution of the phase of junction 1 (black line) and the phase of the center of masses of the fluxon (gray line) divided by $2\pi$ at $i = 0.005, 0.01, 0.02, 0.05,$ and $0.07$.

the *I-V* curve. Looking at *I-V* curves, it appears that the switching current value is defined by some value of the fluxon velocity. Comparing the standard deviation curve in Fig. 9 to the similar one with the lower threshold in Fig. 4, as expected, we can see that a peak occurs much earlier in temperature for the jump from the diffusion state.

## IV. DISCUSSION AND CONCLUSIONS

We have studied the thermal depinning of fluxons in small Josephson rings at small values of damping. At zero tem-
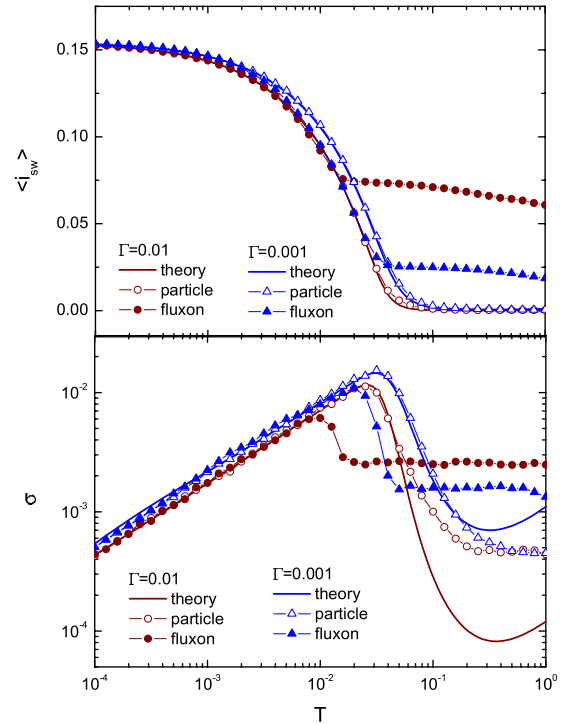


FIG. 9. (Color online) $\langle i_{\text{sw}} \rangle$ and $\sigma$ as a function of $T$ at $\lambda = 0.4$ for two different values of the damping $\Gamma = 0.01$ and 0.001. We show plots for the theoretical prediction (solid line), the particle (open symbols), and the fluxon (solid symbols).

perature, as current is increased, the system switches from a superconducting zero-voltage state to a resistive state where $v = i$. This happens at the so-called depinning current. Beyond this current there is no static configuration for one fluxon in the array, and the fluxon starts to move. Due to the low value of the damping, when fluxon goes through the array, it causes the junctions to switch to a high-voltage state. Then all the junctions do the same but with a phase difference that accounts for the presence of one quantum of flux that is homogeneously distributed along the whole array.

Due to thermal fluctuations, in experiment, the value of the measured depinning current changes from one *IV* to another and only a probability distribution function has sense. This function is usually characterized by its mean value and its standard deviation. The main objective of this paper has been to numerically study how these observables behave for different system parameters (coupling $\lambda$, damping $\Gamma$, and temperature $T$).[29] We have also compared these results with numerical simulations and theoretical estimations for the depinning of a single particle in a sinusoidal potential.

As expected, the mean value of the depinning or the switching current decreases as temperature is raised. At low temperatures the standard deviation follows the usual $T^{2/3}$ law. At higher temperatures the $\sigma(T)$ function reaches a peak that we can identify with the points on the $\langle i_{\text{dep}}(T) \rangle$ or $\langle i_{\text{sw}}(T) \rangle$ curves at which the curvature changes sign (inflection point).

Roughly speaking our results show that the depinning of the fluxon can be understood in terms of the stochastic dynamics of a single particle in a tilted sinusoidal potential.

However, we have seen some unexpected effects that we attribute to discreteness. For the case of small coupling ($\lambda$ =0.4 and smaller) we have seen an increasing deviation of the fluxon depinning behavior from our expectations from the single-particle picture. Arrays with a larger coupling are closer to the continuous limit and discreteness effects are smaller; here the single-particle picture works much better.

The other effect we have observed is the emergence at small damping of a low-voltage thermally excited state that we call fluxon diffusion. In such cases the zero-temperature *I-V* curve does not show any resonance or low-voltage state, and the system switches from zero voltage to the high-voltage branch. However, after some temperature a low-voltage branch is observed. The system first switches from zero to this branch and then to the high-voltage state. At higher temperatures the system first continuously increases voltage from zero (then it is not clear how to define $i_{dep}$), and at larger currents it switches from the low-voltage state to the high-voltage one. We have also seen that the values of damping and current for which this behavior is observed depend importantly in $\lambda$ and also in the number of junctions in the array, $N$.[30]

An important point of our work has been comparing our numerical results with results based on the single-particle picture. The main conclusion is that for most of the cases this picture gives a good estimation of the fluxon depinning current. In fact, in an experimental case, where the different parameters (mainly $\lambda$, $\Gamma$, and $I_c$) are known with some imprecision, it will be difficult to identify deviations from the expected behavior. In addition, there are some points that are difficult to address: the effective one-dimensional potential for the fluxon in the array (Peierls-Nabarro potential) is not purely sinusoidal, and the value of the fluxon mass is not constant since it depends on the fluxon position and the current value. We are also neglecting all the system degrees of freedom except one, and we know that in some cases this is not valid: for instance, in understanding resonant steps which are due to coupling between the fluxon velocity and the linear waves of the discrete array or in understanding the fluxon diffusion branch. We have also considered the expression for the escape rate in a multidimensional case. In this expression, usually, the attempt frequency depends on the frequency of all the stable modes in the minimum and the saddle.[25] We have computed such numbers and checked that the maximum error is smaller than 7% (and occurs for $\lambda$ =0.125).

Our numerical results for the single particle agree pretty well with the predictions from Kramers theory for escape rate except for some limits. Disagreement at high temperatures is expected since theoretical expressions are computed in the infinite barrier limit of the system ($E_b \gg kT$). This limit is not fulfilled at high temperatures. This is also true at small temperatures, where most of the escape events occur at currents very close to $i_{dep}$ where the barrier is also very small. We have checked that the $E_b/kT$ ratio in this case is also small. To finish we have to mention the unexpected disagreement at small values of $\Gamma$. We are currently studying further such results.

In this paper, we have presented results for the mean value and standard deviation of the fluxon depinning current
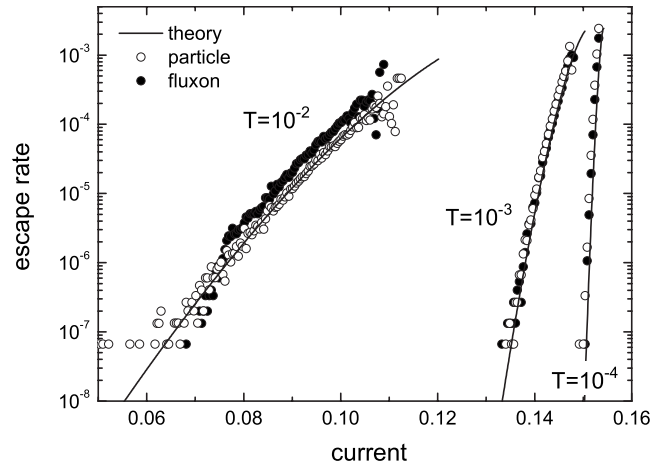


FIG. 10. Escape rate as a function of the current at three different temperatures ($1 \times 10^{-2}$, $1 \times 10^{-3}$, and $1 \times 10^{-4}$) for $\lambda$=0.4 and $\Gamma$=0.01.

probability distribution. It is also possible to describe the data in terms of an escape rate, which is a magnitude that does not depend on experimental details such as the ramp rate of the current. Escape rate can be easily computed from this probability distribution function.[21] A good statistic is usually required to have satisfactory results. For a limited number of temperatures we have computed depinning current values for 10 000 samples and extracted from the results the escape rate values. Results are shown in Figs. 10 and 11. As expected from Figs. 4 and 5, the agreement between numerical results for the fluxon and the particle and theory is excellent at $\lambda$=0.8 and at $\lambda$=0.4 and low temperatures. The fluxon results slightly deviate at $\lambda$=0.4 and $T$=0.01, which is close to the region with a fluxon diffusion branch. We have also computed (Fig. 12) the probability distribution function and escape rate for the switching from the low-voltage fluxon diffusion state to the high-voltage whirling mode, see also Fig. 9.

In the single-particle picture, or the resistive and capacitively shunted junction (RCSJ) model for a single junction, it has become generally accepted that diffusion cannot coexist
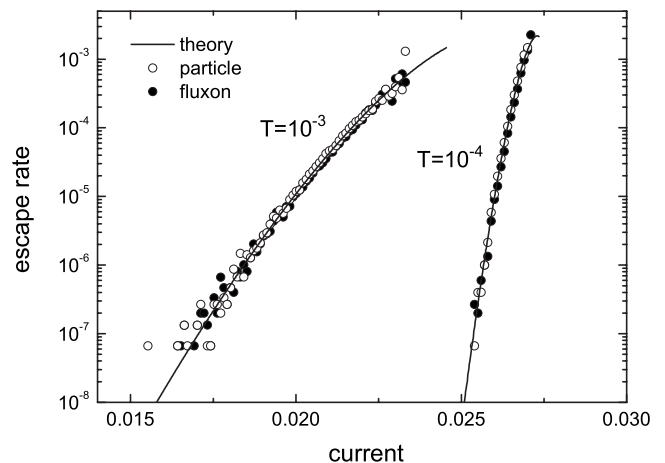


FIG. 11. Escape rate as a function of the current at two different temperatures ($1 \times 10^{-3}$ and $1 \times 10^{-4}$) for $\lambda$=0.8 and $\Gamma$=0.01.
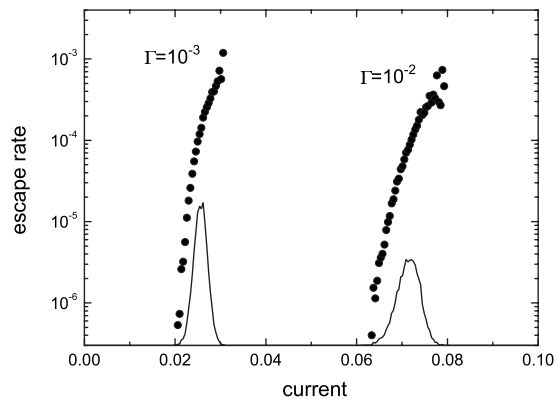
FIG. 12. Escape rate and probability distribution function for the switching from the fluxon diffusion branch. $\lambda = 0.4$, $\Gamma = 0.01$ and 0.001, and $T = 0.1$.

with hysteresis. This was elucidated nicely in Kautz and Martinis[31] through phase-space arguments. Simply put, if the value of applied current is sufficient to allow a stable running state to coexist with the fixed points of zero voltage, the basins of attraction for that running state necessarily separates the basins of attraction for any two neighboring fixed points. Phase jumps between two fixed points are thus forbidden, as the system must first pass through the basin of attraction for the running state. While we have shown in the previous section that the initial escape of the fluxon from its minima can be explained by thermal activation of a single particle, the fluxon diffusion state in the $I$-$V$ curves of Fig. 2 cannot be explained in a similar way.

In the original single-junction experiments on phase diffusion, the coexistence of phase diffusion and hysteresis was explained by the presence of frequency-dependent damping from the junction leads. A simple model of frequency-dependent damping is a series $RC$ circuit in parallel with the junction, which adds an extra degree of freedom to the phase space for the junction dynamics. This extra dimension re-

solves the above-mentioned issue regarding the nonoverlapping basins of attraction. The main result of the paper is the observation of fluxon diffusion in our simulations without frequency-dependent damping, which has not been included in our equations. Instead of the extra dimension introduced by frequency-dependent damping, fluxon diffusion must occur because of the additional degrees of freedom from the multiple junctions in the array. We plan to explore the physics of this different diffusion mechanism in future experiments and simulations.

When studying the behavior of the system at different temperatures we have seen that the mean value of the distribution of the switching current from the fluxon diffusion branch is almost constant, and the standard deviation is very small. Comparing the standard deviation curve in Fig. 9 to the similar one with the lower threshold in Fig. 4, we also see that a peak occurs much earlier in temperature for the jump from the diffusion state. This peak in the standard deviation is also reminiscent of experiments on single junctions,[32–34] where a peak in the standard deviation indicated the collapse of thermal activation and the onset of diffusion.

To finish we want to mention that to our knowledge there are no experimental or numerical results studying systematically the thermal escape of fluxons or solitons in discrete arrays. However we want to mention here the work of Wallraff *et al.*[35] on vortices in long JJ. With respect to theoretical advances we also want to cite a recent work[36] where major differences between the macroscopic quantum tunneling in long JJs from tunneling of a quantum particle are reported.

## ACKNOWLEDGMENTS

[1] M. Remoissenet, *Waves Called Solitons: Concepts and Experiments* (Springer, Berlin, 1994).

[2] A. C. Scott, *Nonlinear Science: Emergence and Dynamics of Coherent Structures*, 2nd ed. (Oxford University Press, Oxford, 2003).

[3] O. M. Braun and Y. S. Kivshar, Phys. Rep. **306**, 1 (1998).

[4] O. M. Braun and Y. S. Kivshar, *The Frenkel-Kontorova Model* (Springer, New York, 2004).

[5] L. M. Floría and J. J. Mazo, Adv. Phys. **45**, 505 (1996).

[6] K. K. Likharev, *Dynamics of Josephson Junctions and Circuits* (Gordon and Breach, New York, 1986).

[7] M. Tinkham, *Introduction to Superconductivity*, 2nd ed. (McGraw-Hill, New York, 1996).

[8] A. V. Ustinov, Physica D **123**, 315 (1998).

[9] S. Watanabe, H. S. J. van der Zant, S. H. Strogatz, and T. P. Orlando, Physica D **97**, 429 (1996).

[10] K. Segall, A. P. Dioguardi, N. Fernandes, and J. J. Mazo, J. Low Temp. Phys., doi:10.1007/s10909-008-9849-8 (2008).

[11] The existence of a depinning current is also a discrete effect (breaking of fluxon translational symmetry). The depinning current rapidly approaches to zero when $\lambda$ increases and we approach the continuous limit of the system.

[12] A. V. Ustinov, M. Cirillo, and B. A. Malomed, Phys. Rev. B **47**, 8357 (1993).

[13] H. S. J. van der Zant, T. P. Orlando, S. Watanabe, and S. H. Strogatz, Phys. Rev. Lett. **74**, 174 (1995).

[14] A. V. Ustinov, M. Cirillo, B. H. Larsen, V. A. Oboznov, P. Carelli, and G. Rotoli, Phys. Rev. B **51**, 3081 (1995).

[15] S. Watanabe, S. H. Strogatz, H. S. J. van der Zant, and T. P. Orlando, Phys. Rev. Lett. **74**, 379 (1995).

[16] Z. Zheng, B. Hu, and G. Hu, Phys. Rev. B **58**, 5453 (1998).

[17] J. Pfeiffer, A. A. Abdumalikov, M. Schuster, and A. V. Ustinov, Phys. Rev. B **77**, 024511 (2008).

[18] This scaling is based in the normalization of Eq. (2).

[19] P. J. Martínez, F. Falo, J. J. Mazo, L. M. Floría, and A. Sánchez, Phys. Rev. B **56**, 87 (1997).

[20] C. Cattuto, G. Costantini, T. Guidi, and F. Marchesoni, Phys. Rev. B **63**, 094308 (2001).

[21] T. A. Fulton and L. N. Dunkleberger, Phys. Rev. B **9**, 4760 (1974).

[22] J. M. Martinis, M. H. Devoret, and J. Clarke, Phys. Rev. B **35**, 4682 (1987).

[23] M. Büttiker, E. P. Harris, and R. Landauer, Phys. Rev. B **28**, 1268 (1983).

[24] V. I. Mel'nikov and S. V. Meshkov, J. Chem. Phys. **85**, 1018 (1986).

[25] P. Hänggi, P. Talkner, and M. Borkovec, Rev. Mod. Phys. **62**, 251 (1990).

[26] V. I. Mel'nikov, Phys. Rep. **209**, 1 (1991).

[27] This value is given by H. Risken and K. Voigtlaender, J. Stat. Phys. **41**, 825 (1985). It also corresponds to the number which at low damping gives the better agreement between the Büttiker, Harris, and Landauer equation and the Mel'nikov and Meshkov one.

[28] Note that the $T/i_{\text{dep}}^0$ ratio is the same for both cases.

[29] This value also depend on the current ramp which enters into the equations in a way well established by theory.

[30] This paper only shows results for 9 junctions arrays. However, we have done also numerical simulations for larger arrays.

[31] R. L. Kautz and J. M. Martinis, Phys. Rev. B **42**, 9903 (1990).

[32] J. M. Kivioja, T. E. Nieminen, J. Claudon, O. Buisson, F. W. J. Hekking, and J. P. Pekola, Phys. Rev. Lett. **94**, 247002 (2005).

[33] V. M. Krasnov, T. Bauch, S. Intiso, E. Hürfeld, T. Akazaki, H. Takayanagi, and P. Delsing, Phys. Rev. Lett. **95**, 157002 (2005).

[34] J. Männik, S. Li, W. Qiu, W. Chen, V. Patel, S. Han, and J. E. Lukens, Phys. Rev. B **71**, 220509(R) (2005).

[35] A. Wallraff, J. Lisenfeld, A. Lukashenko, A. Kemp, M. Fistul, Y. Koval, and A. V. Ustinov, Nature (London) **425**, 155 (2003); A. Wallraff, A. Lukashenko, C. Coqui, A. Kemp, T. Duty, and A. V. Ustinov, Rev. Sci. Instrum. **74**, 3740 (2003).

[36] A. O. Sboychakov, S. Savel'ev, A. L. Rakhmanov, and F. Nori, Europhys. Lett. **80**, 17009 (2007).